

Performance and Analysis of BLDC Motor Using ANSYS Maxwell Software

K.Arun¹, Yugeshvar.V², Riyas Ahamed.A³, Suvedharan.V⁴, Shri Vignesh .B⁵

¹Associate Professor, EEE Dept., SMVEC, Puducherry.

^{2,3,4,5}UG Scholar, EEE Dept., SMVEC, Puducherry.

Abstract – This paper is about the simulation of a Brush-Less Direct Current Machine in the ANSYS – Maxwell Environment. The machine is selected for a high-performance electric-bike as a motor over the UNEP (United Nations Environment Program) metropolitan drive cycle. Analytical study of the forces influencing the machine along with industry references and literature review led to estimation of rated operating parameters. Four models of a 1,500Watt, 380Rpm, 40Nm & 48Volt BLDC Motor are designed and simulated in the RMXprt module of Maxwell [24 Slot, 36 Slot, 48Slot & 72 Slot] The software enabled solving and simulation of magneto-static and transient fields based on Maxwell's equations in 2D & 3D. All machines are at an efficiency of 85% - 88% while operating under rated parameters and are operating in the end region of the torque and power curve. All machines are capable of 5kW – 6kW peak power output at 150Rpm – 250 Rpm. It may be said that, precise designing of winding dimensions may lead to further increase in efficiency. The solution set of each machine is described and tabulated in the appendix of this thesis. 2D and 3D analysis reveals inconsistencies in the waveform of torque, winding currents, induced voltages and losses of 36 Slot Machine, while other machines have acceptable wave form characteristics. Field plots show nominal magnetic field density in stator teeth with few tolerable hot spots for all the machines. Field overlays show higher than expected current density in the stator sections of all machines. Overall the 24, 48 and 72 Slot machine suit best for the given application.

Key Words: ANSYS, BLDC Motor, Maxwell Software.

1. INTRODUCTION

Brushless dc motors are popular in a wide range of industrial applications, such as computer peripherals, servo control systems and electrical tools due to their robustness, simplicity, large torque to volume ratio and high-efficiency. Interior permanent magnet brushless DC (IPMBLDC) electric motor is an important category of these motors, constructed with the permanent magnets inserted into the steel rotor core and does not need to be glued such as in surface mounted permanent magnet motors. The leakage path of interior magnet motors usually includes a saturable magnetic bridge and the web, which will make the coefficient of flux leakage variable. Some studies have been done on Brushless direct current motor (BLDC) design for different applications at different power levels. However, most of them used the computer-aided tools and experience to get the BLDC motor parameters, which usually takes time. In this paper, we are going to introduce a quantitative model to obtain the initial BLDC motor parameters. Then

the MAXWELL 2D finite element method (FEM) is used to optimize all the initial design parameters, which will give guidance for the BLDC motor design and reduce the design time. The electric impact wrench motor application is different from the regular applications that incorporate motors working with a continuous model. The impact wrench motor works with a discontinuous model, which requires high reliability, small size, less bolting time, low cost, high pull-out torque to load and unload car bolts in a short time and to enable industrial mass production. In this paper, a much lower torque angle is selected at the rated power and speed in the design. Such a design can effectively increase the overload handling capability and provide high torque at a short time.

This paper presents an analytical method to design the interior permanent magnet brushless DC motor with concentrated windings block and applied in the impact wrench. The assumed flux leakage coefficient and working point of a selected permanent magnet are used in the initial design. The equivalent magnetic circuit of IPMBLDC motor is built to calculate the coefficient of flux and working point of a permanent magnet based on the design output parameters.

A computer-aided tool is used to calculate and compare the calculated values and hypothesis values. Structure parameters will be adjusted based on the error between the assumed and the calculated value. A new mechanical structure of the impact wrench is designed, and its working principle is analyzed in detail. The motor connects to a planetary gear reducer with a transmission ratio to get high output torque. Hence, the speed of impact wrench will be reduced. The bolting time is related to motor speed, main pressure spring as well as shock block. The motor is required to get high load capability and improve lifetime. The new impact wrench mechanical structure is simple, has a small volume, and is lightweight and easy to use. It can substantially reduce labor intensity and improve work efficiency.

Maxwell 2D FEM is used to verify the equivalent magnetic circuit and optimize the design of the IPMBLDC motor. Thermal analysis is carried out with the aid of Motor Solve packages. The working principle, the planetary gear reduce transmission ratio formula as well as the dynamic model of the main pressure spring and shock block in the impact process is introduced. The whole electric impact wrench has been designed and fabricated. Experiment results are obtained to verify the design.

This paper is organized in the following sections: Section 2 focuses on the motor design process. Section 3 then looks at the impact wrench mechanical system design and calculation. Sections 4 and 5 proceeds to show associated simulation analysis as well as experimental results. Finally, the conclusion and remarks are given in Section 6.

2. LITERATURE SURVEY

Jang, S.M.; Cho, H.W.; Choi, S.K. Design and Analysis of a High-Speed Brushless DC Motor for Centrifugal Compressor. *IEEE Trans. Magn.* 2007, 43, 2573-2575. This paper describes the design and analysis of a high-speed and high-power density BLDC motor for a 50-kW, 70 000-rpm class centrifugal compressor. Design criteria and power loss analysis of the high-speed machine structure are described by analytical method, and the results are validated by finite element method.

He, C.; Wu, T.; Wu, W.; Chow, L.; Harms, J.; Taylor, D.R. Design, analysis and experiment of a high efficiency permanent magnet truck alternator. In Proceedings of the 43rd Annual Conference of the IEEE Industrial Electronics Society (IECON 2017), Beijing, China, 29 October-1 November 2017. In recent years, renewable green energy has increased the demand associated with the development of high efficiency electrical permanent magnet synchronous machinery. The electrical motors consume more than half of all electrical energy in the state according to the U.S. Department of Energy. Therefore, designing a high-efficiency energy conversion device and its control system becomes critical. Permanent magnet synchronous motor (PMSM) and Permanent magnet synchronous generator (PMSG) can be such energy conversion device.

Seol, H.S.; Kang, D.W.; Jun, H.W.; Lim, J.; Lee, J. Design of Winding Changeable BLDC Motor Considering Demagnetization in Winding Change Section. *IEEE Trans. Magn.* 2017, 53, 1-5. The changeable winding BLDC motor is driven by a large number of phase turns at low speeds and by a reduced number of turns at high speeds. For this reason, the section where the winding changes is very important. Ideally, the time at which the windings are to be converted should be same as the time at which the voltage change.

Feng, J., Liu, K., Wang, Q. Scheme based on buck-converter with three phase Hbridge combinations for high-speed BLDC motors in aerospace applications, *IET Electr. Power Appl.* 2018, 12, 405-414. Considering the aerospace applications, different types of motors can be used in the control moment gyroscope. gyro is an attitude control device used in the attitude control system. Due to the different advantages of brushless dc (BLDC) .motors like high power density, higher efficiency, high dynamic response, linear speed torque characteristics and long life it is more preferred than all other motors in aerospace applications. As this paper deals with a critical application like spacecraft, reliability of the system is the first concern.

Li, H.; Li, W.; Ren, H. Fault-tolerant inverter for high-speed low-inductance BLDC drives in aerospace

applications. *IEEE Trans. Power Electron.* 2017, 32, 2452–2463. The fault-tolerant control of the BLDC motor is of great importance for its continuous operating capacity even under the faulty situation. This paper proposes a fault-tolerant topology composed of an additional phase leg and a fault-protective circuit for the high-speed low-inductance BLDC motor. Based on the analysis of the overcurrent and overvoltage phenomenon after the switch faults, a novel fault isolation and system reconfiguration method is presented.

Batzel, T.D.; Lee, K.Y. Electric Propulsion with Sensor less Permanent Magnet Synchronous Motor: Implementation and Performance. *IEEE Trans. Energy Convers.* 2005, 20, 575–584. There has recently been considerable interest in using the sensor less permanent magnet synchronous motor (PMSM) for vehicle propulsion systems. While many sensor less PMSM techniques have been presented in the literature, few have discussed in detail the underlying hardware and implementation issues.

Ko, J.-S.; Choi, J.-S.; Chung, D.-H. Maximum Torque Control of an IPMSM Drive Using an Adaptive Learning Fuzzy-neural Network. *J. Power Electron.* 2012, 12, 468–477. This paper presents an analytical method to design an interior permanent magnet brushless DC electric motor (IPMBLDC motor) for a kind of electric impact wrench used for loading and unloading car bolts. It takes into account magnet assembly gap, rotor saturation webs, and bridges.

Kim, K.-T.; Kim, K.-S.; Hwang, S.-M.; Kim, T.-J.; Jung, Y. Comparison of Magnetic Forces for IPM and SPM Motor with Rotor Eccentricity. *IEEE Trans. Magn.* 2001, 37, 3448–3451. The derived formula predicts the UMP making use only of the magnet permanent flux density, rotor eccentricity, and geometrical parameters of the motor. The formula was discussed and compared with measurement data. Except of the UMP the eccentricity-dependent magnetic stiffness coefficient has been derived and presented in figures as a function of the ratio of the airgap length to the magnet height. It could be showed that in the case of examined PM machines, the magnetic stiffness coefficient varies quite moderate with the rotor eccentricity.

Sashidhar, S.; Fernandes, B.G. Braking Torque Due to Cross Magnetization in Unsaturated IPM BLDC Machines and Its Mitigation. *IEEE Trans.* 2017, 53, doi:10.1109/TMAG.2016.2618343. Cross magnetization (CM) is an inevitable phenomenon in electrical machines. It is more prominent in interior permanent magnet (IPM) brushless dc (BLDC) machines. This is because PMs demagnetize in overloaded and saturated conditions. It leads to cross coupling between the direct and quadrature-axes quantities, and a decrease in the resultant air-gap flux-density distribution under saturated conditions.

Fan, Y.; Li, C.; Zhu, W.; Zhang, X.; Zhang, L.; Cheng, M. Stator Winding Inter-turn Short Circuit Faults Severity Detection Controlled by OWSVPWM without CMV of Five-phase FTFSCW-IPM. *IEEE Trans. Ind. Appl.* 2017, 53, 194–202. The impact of a harsh operational environment most often leads to faults in PM machines. The diagnosis and

nipping of such faults at an early stage have appeared as the prime concern of manufacturers and end users. This paper reviews the recent advances in fault diagnosis techniques of the two most frequently occurring faults, namely inter-turn

short fault (ITSF) and irreversible demagnetization fault (IDF). ITSF is associated with a short circuit in stator winding turns in the same phase of the machine, while IDF is associated with the weakening strength of the PM in the rotor.

3. PMBLDC MOTOR STRUCTURE CONSIDERATION

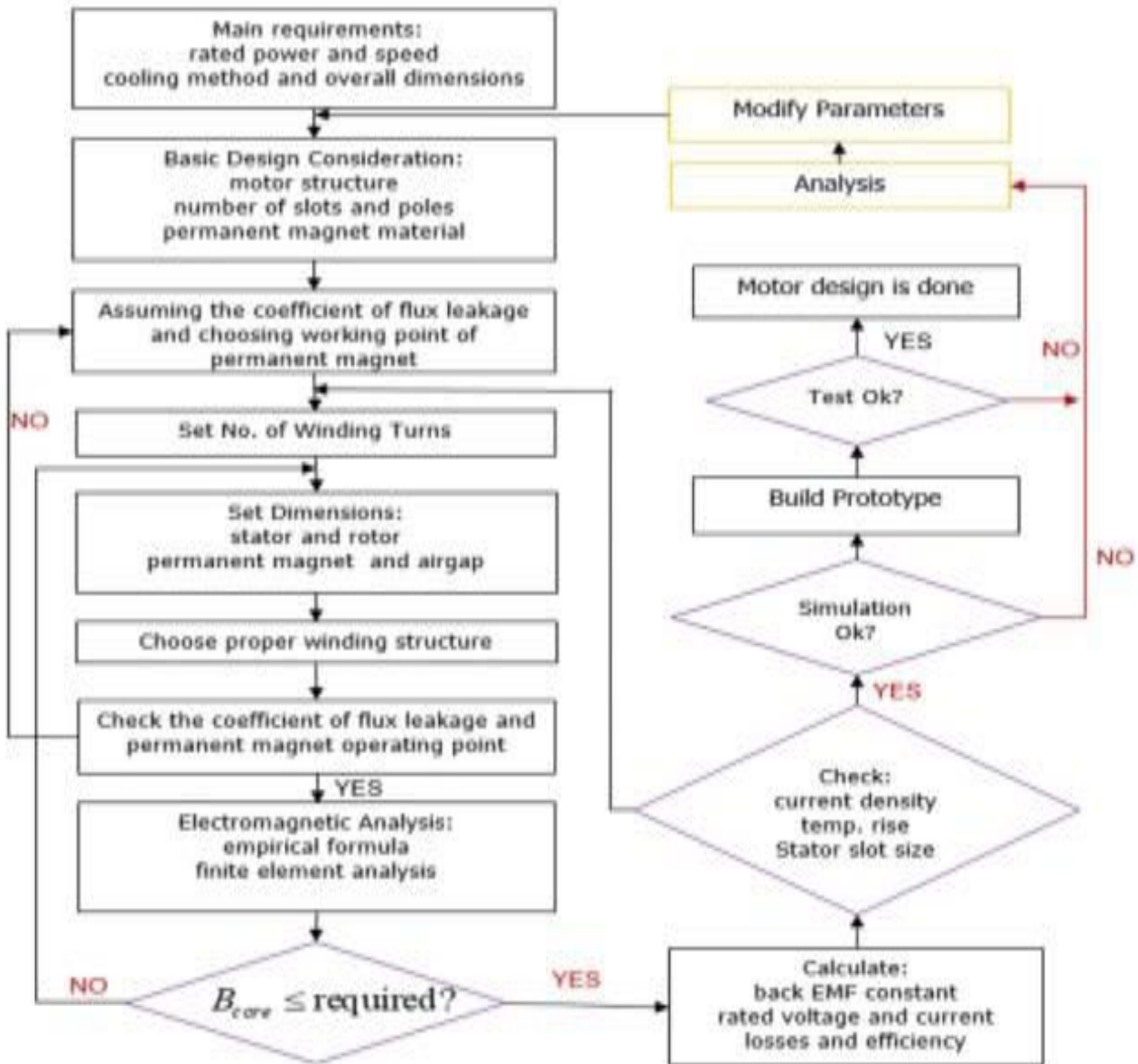


Fig -1: Brushless DC motor design flow.

3.1 Design Parameter

ROTOR

Name	Value	Unit	Evaluated Value	Description
DiaGap	160.4	mm	160.4mm	"Core diameter on gap side, or outer diameter"
DiaYoke	110.64	mm	110.64mm	"Core diameter on yoke side, or inner diameter"
Length	0	mm	0mm	"Core length"
Poles	8		8	"Number of poles"

PoleType	3		3	"Pole type: 1 to 3."
D1	157.44	mm	157.44mm	"Limited diameter of PM ducts"
O1	3	mm	3mm	"Bottom width for separate or flat-bottom duct"
O2	7.28	mm	7.28mm	"Distance from duct bottom to shaft surface"
B1	4.7	mm	4.7mm	"Duct thickness"
Rib	14	mm	14mm	"Rib width"
HRib	3	mm	3mm	"Rib height"
DminMag	4.5	mm	4.5mm	"Minimum distance between side magnets"
ThickMag	6.48	mm	6.48mm	"Magnet thickness"
WidthMag	32	mm	32mm	"Total width of all magnet per pole"
LenRegion	200	mm	200mm	"Region length"
InfoCore	0		0	"0: core; 1: magnets; 2: ducts; 100: region."

STATOR

Name	Value	Unit	Evaluated Value	Description
DiaGap	161.9	mm	161.9mm	"Core diameter on gap side, DiaGap<DiaYoke for outer cores"
DiaYoke	269.24	mm	269.24mm	"Core diameter on yoke side, DiaYoke<DiaGap for inner cores"
Length	0	mm	0mm	"Core length"
Skew	0	deg	0deg	"Skew angle in core length range"
Slots	48		48	"Number of slots"
SlotType	2		2	"Slot type: 1 to 6"
Hs0	1.03	mm	1.03mm	"Slot opening height"
Hs01	0	mm	0mm	"Slot closed bridge height"
Hs1	0	mm	0mm	"Slot wedge height"
Hs2	29.5	mm	29.5mm	"Slot body height"
Bs0	1.93	mm	1.93mm	"Slot opening width"
Bs1	5	mm	5mm	"Slot wedge maximum width"
Bs2	8	mm	8mm	"Slot body bottom width, 0 for parallel teeth"
Rs	5	mm	5mm	"Slot body bottom fillet"
FilletType	0		0	"0: a quarter circle; 1: tangent connection; 2&3: arc bottom."
HalfSlot	0		0	"0 for symmetric slot, 1 for half slot"
SegAngle	0	deg	0deg	"Deviation angle for slot arches (10~30, <10 for true surface)."
LenRegion	200	mm	200mm	"Region length"
InfoCore	0		0	"0: core; 100: region."

DESIGN CALCULATION DETAILS

Name	Value	Unit	Evaluated Value
Poles	8		8
PolePair	Poles/2		4
speed_rad	3000		3000
Thet_deg	20	deg	20deg

Omega	$360 * \text{speed_rad} * \text{PolePair} / 60$		72000
Omega_rad	$\text{Omega} * \pi / 180$		1256.6370614359
Thet	$\text{Thet_deg} * \pi / 180$		0.34906585039887deg
Imax	250	A	250A

4. FINITE ELEMENT METHOD

There are number of techniques which have been developed to solve electromagnetic related problems not amenable to exact solution. The Finite element method is used to convert the complex partial differential equation into nonlinear algebraic equation the finite element method can be applied to the vector Helmholtz wave equation, which is derived from the Maxwell’s equations, or it can be derived from a scalar-vector potential formulation of the fields. There are variety of commercial geometrical modelling tools to accurately model any three-dimensional geometry and to generate the required mesh with any kind of elements such as triangles, tetragonals and hexagonal

FEM involves the following for the solving a boundary value problem:

- i) Discretization of the domain
- ii) Derivation of the element equations
- iii) Assembly of the elements
- iv) Solutions of the system equations.

The field analysis using FEM has three steps

- i. Pre-processing stage
- ii. Processor stage
- iii. Postprocessor stage

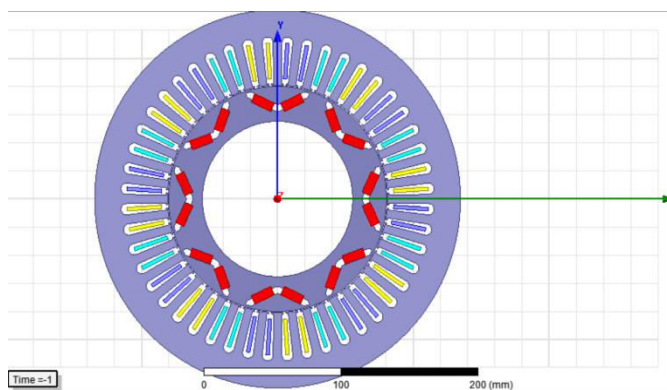


Fig -2: Model Design Of PMBLDC Motor Using Ansoft Maxwell

4.2 Basic Mathematical Formulas Used In Electromagnetic Field

In magnetic field numbers of quantities are used. They are interrelated with each other. Magnetic flux (ϕ) in magnetic field is very similar to electric current (I) in electric field.

Magnetic flux is related with magnetic field density (B) as

$$\phi = B.A \tag{1}$$

Here A is the area of the magnetic flux path. Magnetic flux unit is weber and the unit of magnetic field density is weber/m².

Magnetic flux can be calculated with magneto-motive force (F) and reluctance(R) of the path.

$$F = NI \tag{2}$$

Where N is the number of turns used and I is the current that flow through the coil then

$$\phi = F/R \tag{3}$$

Using equation (2) equation (3) can be represented

$$\phi = NI/R \tag{4}$$

Reluctance of the magnetic path is depends on length of the magnetic path (l), permeability of magnetic material(μ) and area of flux flowing path .

$$R = l/\mu A \tag{5}$$

Magneto-motive force (F) in magnetic circuit is similar to electromotive force (E) in electric circuit. Magnetic field density (B) is similar to electric field density(D)

Maxwell’s equations represent one of the most elegant and concise way to explain the fundamentals of the electricity and magnetism. With the help of Maxwell’s equations one can develop most of the working relationship in static or time varying electromagnetic field.

4.3 Proposed Model of 2D of BLDC Motor using The Material M19_29G

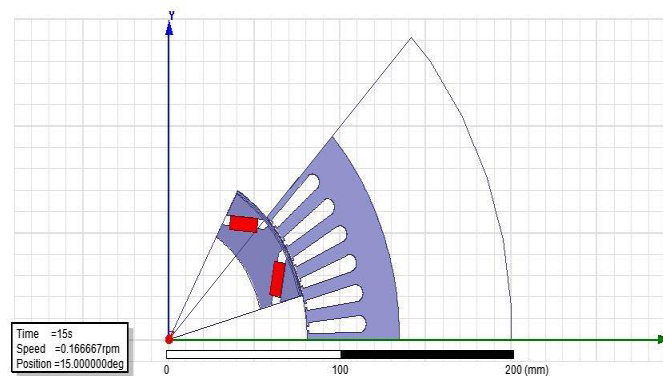


Fig -3: BLDC Motor Using Material M19_29G

ANSYS Maxwell is a comprehensive electromagnetic field simulation software for engineers tasked with designing and analysing 3D/2D structures, such as motors, actuators, transformers and other electric and electro-mechanical devices. ANSYS Maxwell can solve static, frequency-domain and time-varying electromagnetic and electric fields.

4.4 Graphical Analysis of Cogging Torque using Material M19_29G(1.50NM)

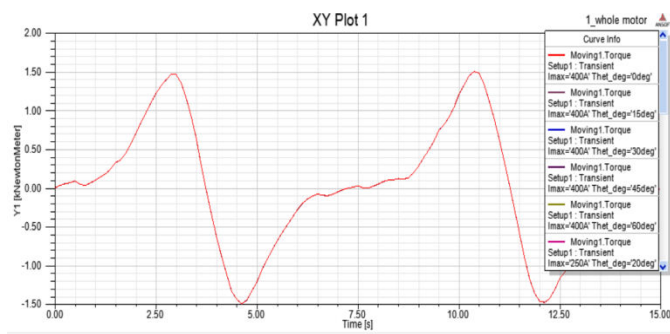


Fig -4: Moving Torque vs Time(cogging torque of M19_29G)

The above graph represents the cogging torque of the motor. X-axis represents the time[s] and Y-axis represents cogging torque of the motor[KNM]

4.5 Graphical Analysis of Current

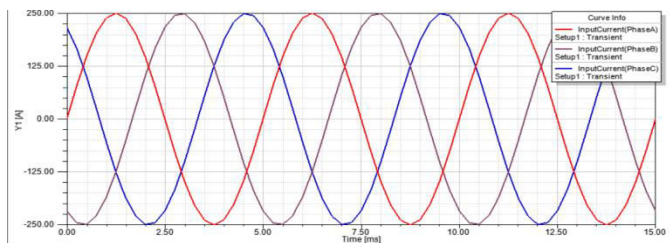


Fig -5: Current vs Time(ms)

The above graph represents the current of the motor. X-axis represents the time[ms] and Y-axis represents Phase A,B and C of the motor[A]

4.6 Graphical Analysis Of Moving Torque

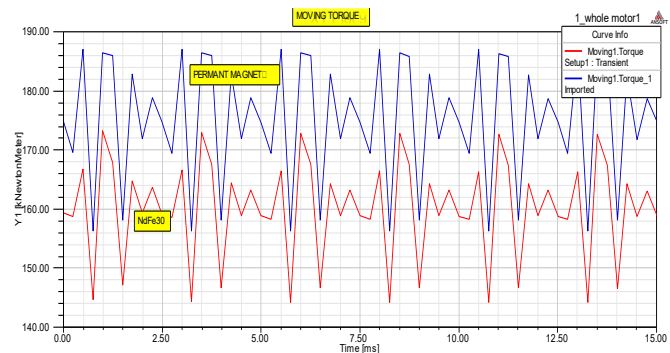


Fig -6: Torque vs Time(ms).

The above graph represents the Moving Torque of the motor. X-axis represents the time[ms] and Y-axis represents Moving Torque of the motor[kNM].

4.7 Graphical Analysis Of Flux Linkages Of Phase A, Phase B, Phase C:

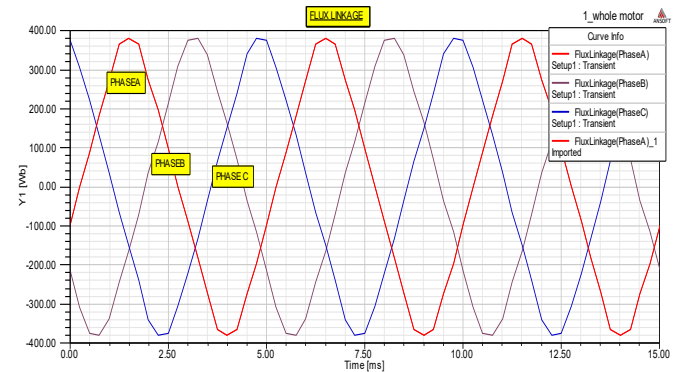


Fig -6: Flux Linkages vs Time(ms)

The above graph represents the Flux Linkages of Phase A,B and C of the motor. X-axis represents the time[ms] and Y-axis represents Flux Linkages Phase A,B and C of the motor[Wb].

4.8 Graphical Analysis of Core Loss

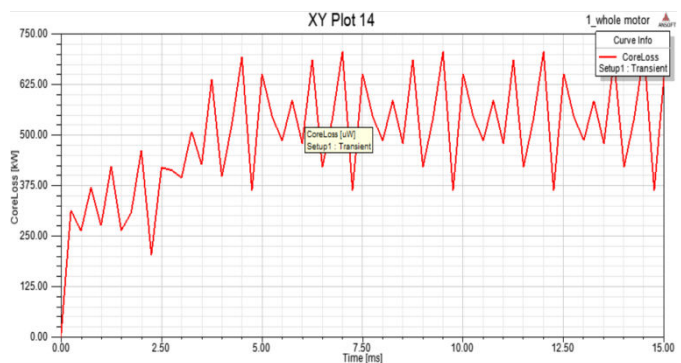


Fig -7: CoreLoss(KW) vs Time(ms)

The above graph represents the Flux Linkages of Phase A,B and C of the motor. X-axis represents the Time[ms] and Y-axis represents CoreLoss of the motor[kW].

4.9 Graphical Analysis of Frequency & Torque

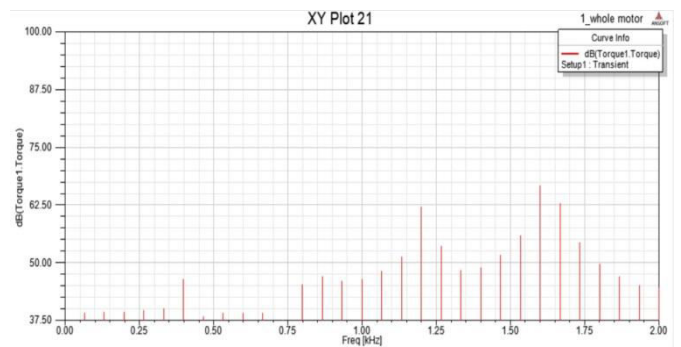


Fig -8: Torque vs Frequency(KHZ).

The above graph represents the torque of the motor. X-axis represents the Frequency[kHz] and Y-axis represents Torque of the motor[dB].

4.10 Graphical Analysis of Induced Voltage

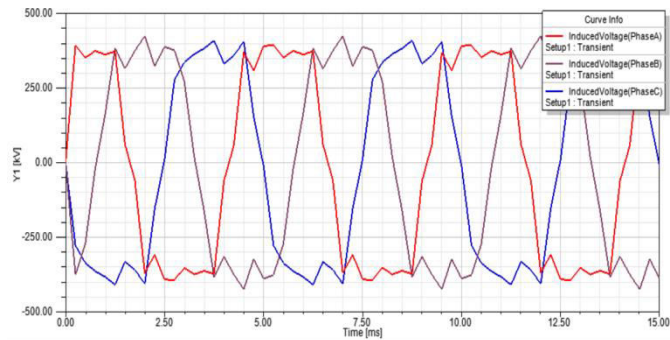


Fig -9: Induced Voltage(KV) vs Time(ms)

The above graph represents the Induced Voltage of the motor. X-axis represents the Time[ms]. and Y-axis represents Induced Voltage of the motor[KV].

4.11 Comparison of Graphical Analysis of Cogging Torque

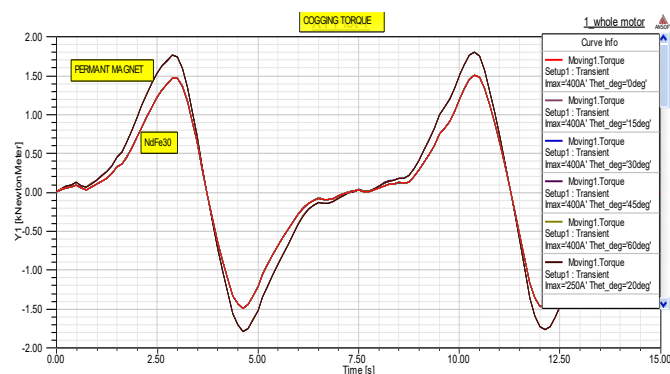


Fig -10: Cogging Torque vs Time(s)

The above graph represents the Cogging Torque of both Material of the motor. X-axis represents the Time[s] and Y-axis represents Cogging Torque of the motor [kNm].

5. CONCLUSION

The basic idea of idea of Permanent Brushless DC Motor. First of all basics of magnetic circuit is explained and then required basic equation used in electromagnetic field is describes. In this paper Permanent BLDC motor used in solar vehicle of 1500W and 3000 rpm is design. This paper shows that motor gives considerably good efficiency at rated speed. Motor is design in RMxprt and its electromagnetic field analysis is done on Maxwell 2D. After designing of motor, analysis is done by varying the lead angle of control circuit. It is seen that when the lead angle is increased from 0 degree to 30 degree efficiency of the Permanent BLDC Motor is increased by increasing lead

angle rated speed of motor is increased. Increase in efficiency is achieved at the cost of decrease in rated torque and increase in ripple in torque.

6. FUTURE SCOPE OF THE PROJECT

As this project is done using Ansys Maxwell Software for designing and analyzing the BLDC motor so we can use this in an economically beneficial way by using thermal analysis we can improve the performance and efficiency of the motor by reducing the flux linkage and current leakage. By differentiating the speed, slot and pole we can acquire many values and results for further improvement in the project. The permanent magnet can also be changed and the design too can be varied by the characteristics with low cost and less man work.

References

- O. Bolton, "Electrical bicycle". Canton, Ohio Patent US 552271 A, 19 September 1895.
- Faulhaber Group, "www.micromo.com," [Online]. Available: http://static.micromo.com/media/wysiwyg/Technical-library/Brushless/Brushless_Application_Advantage_WP.pdf.
- P. T. T.G. Wilson, "D.C. Machine. With Solid State Commutation," *AIEE*, 1962.
- Pushek Madaan, Cypress Semiconductor, "www.edn.com," 11 February 2013. [Online]. Available: <http://www.edn.com/design/sensors/4406682/Brushless-DC-Motors---Part-I---Construction-and-Operating-Principles>.
- H. T. W. I. Muhammad Nizam, "Design of Optimal Outer Rotor Brushless DC for Minimum Cogging Torque," in *Joint International Conference on Rural Information & Communication Technology and Electric-Vehicle Technology (rICT & ICeV-T)*, Bandung-Bali, Indonesia, 2013.
- Beikimco, "www.beikimco.com," [Online]. Available: <http://www.beikimco.com/resources-downloads/about-bldc-motors/what-is-a-brushless-DC-motor>.
- Honeywell, "www.digikey.com," June 2012. [Online]. Available: http://www.digikey.com/Web%20Export/Supplier%20Content/HoneywellSC_480/PDF/honeywell-an-ss-hall-effects.pdf.
- Microchip Technology Inc., "www.microchip.com," 2007. [Online]. Available: <http://ww1.microchip.com/downloads/en/AppNotes/01083a.pdf>.
- Atmel Corporation, "www.atmel.com," 2005. [Online]. Available: <http://www.atmel.com/images/doc8012.pdf>.
- A. Reinap, "Design of Powder Core Motors," Department of Industrial Electrical Engineering and Automation, Lund University, Lund, Sweden, 2004.